RESEARCH ARTICLE

Choriocapillaris reduction accurately discriminates against early-onset Alzheimer's disease

William Robert Kwapong[1] | Fei Tang[2] | Peng Liu[3] | Ziyi Zhang[1] | Le Cao[1] |
Zijuan Feng[1] | Shiyun Yang[1] | Yang Shu[2] | Heng Xu[2] | Ying Lu[2] | Xinjun Zhao[2] |
Baochen Chong[2] | Bo Wu[1] | Ming Liu[1] | Peng Lei[1,2] | Shuting Zhang[1]

[1]Department of Neurology, West China Hospital, Sichuan University, Chengdu, P.R. China

[2]State Key Laboratory of Biotherapy, West China Hospital, Sichuan University, Chengdu, P.R. China

[3]Department of Emergency, West China Hospital of Sichuan University, Chengdu, P.R. China

Correspondence
Shuting Zhang, Department of Neurology, West China Hospital, Sichuan University, No. 37 Guo Xue Xiang, Chengdu 610041, Sichuan Province, P.R. China.
Email: shutingzhang@scu.edu.cn

Peng Lei, Department of Neurology and State Key Laboratory of Biotherapy, West China Hospital, Sichuan University, Chengdu 610041, P.R. China.
Email: peng.lei@scu.edu.cn

Ming Liu, Department of Neurology, West China Hospital, Sichuan University, No. 37 Guo Xue Xiang, Chengdu 610041, Sichuan Province, P.R. China.
Email: wyplmh@hotmail.com

Trial registration number:
ChiCTR2000041386, Chinese Clinical Trial Registry
(https://www.chictr.org.cn/index.html)

Abstract

INTRODUCTION: This study addresses the urgent need for non-invasive early-onset Alzheimer's disease (EOAD) prediction. Using optical coherence tomography angiography (OCTA), we present a choriocapillaris model sensitive to EOAD, correlating with serum biomarkers.

METHODS: Eighty-four EOAD patients and 73 controls were assigned to swept-source OCTA (SS-OCTA) or the spectral domain OCTA (SD-OCTA) cohorts. Our hypothesis on choriocapillaris predictive potential in EOAD was tested and validated in these two cohorts.

RESULTS: Both cohorts revealed diminished choriocapillaris signals, demonstrating the highest discriminatory capability (area under the receiver operating characteristic curve: SS-OCTA 0.913, SD-OCTA 0.991; $P < 0.001$). A sparser SS-OCTA choriocapillaris correlated with increased serum amyloid beta (Aβ)42, Aβ42/40, and phosphorylated tau (p-tau)181 levels (all $P < 0.05$). Apolipoprotein E status did not affect choriocapillaris measurement.

DISCUSSION: The choriocapillaris, observed in both cohorts, proves sensitive to EOAD diagnosis, and correlates with serum Aβ and p-tau181 levels, suggesting its potential as a diagnostic tool for identifying and tracking microvascular changes in EOAD.

KEYWORDS
amyloid beta, choriocapillaris, early-onset dementia, retinal microvasculature, tau

---

William Robert Kwapong, Fei Tang, and Peng Liu contributed equally to this work.

Highlights

- Optical coherence tomography angiography may be applied for non-invasive screening of Alzheimer's disease (AD).
- Choriocapillaris demonstrates high sensitivity and specificity for early-onset AD diagnosis.
- Microvascular dynamics abnormalities are associated with AD.

1 | BACKGROUND

Alzheimer's disease (AD) represents a significant challenge in clinical medicine as disease-modifying therapy is limited. Clinical trials have failed to demonstrate efficacy in halting disease progression, possibly due to a focus on patients in the advanced stages of the disease.[1] Considering the disease duration of AD can be decades, it exhibits a lengthy asymptomatic preclinical stage marked by various pathological changes, necessitating effective, easy-to-use markers for early-stage AD screening.

Vascular changes have been identified as important contributors to AD pathogenesis.[2–4] However, in vivo visualization of cerebral microcirculation remains a challenge.[5–7] A viable solution is retinal imaging, proposed as a means of assessing pathological brain changes due to shared embryological origins and microvasculature between the retina and the brain.[8] Given that decreased cerebral blood flow is a precursor to dementia,[9] retinal microvasculature may serve as an effective biomarker for disease screening.

Retinal microvasculature can be assayed using optical coherence tomography angiography (OCTA). The choroid is a layer of the eye located between the retina and the outer layer of the eye, which is responsible for the majority of blood supply to the retina, including the retinal pigment epithelium (RPE) and photoreceptors, as well as some portions of the inner retina.[10] Due to its sensitivity and close relationship with the macula, the choriocapillaris could be considered the most sensitive microvascular structure of the fundus (Figure S1 in supporting information). Individuals with dementia exhibit thinner choroidal structure/thickness compared to control subjects,[11–13] suggesting the presence of an abnormal choroidal blood supply. Furthermore, the retinal choroid has been proposed as an early ocular marker of neurodegeneration in the brain, potentially offering greater reliability than traditional retinal structural thinning assessments.[11,13–15] While both swept-source OCTA (SS-OCTA) and spectral domain OCTA (SD-OCTA) can detect choroidal blood supply, SS-OCTA might demonstrate more sensitivity due to its faster scanning speed and longer wavelength.

Early-onset AD (EOAD)[16] diagnosed in those < 65 years offers a promising avenue for identifying diagnostic indicators potentially applicable to sporadic AD.[17,18] Using SD-OCTA, our previous study identified a relationship between choriocapillaris and cognitive function in EOAD patients.[19] Building upon this, we further investigated the relationship between choriocapillaris and blood biomarkers using two types of OCTA (SS-OCTA and SD-OCTA). We used a discovery cohort of SS-OCTA to explore the predictive capabilities of the choriocapillaris in EOAD. Subsequently, we validated this discovery in the SD-OCTA cohort. We have examined retinal microvasculature and choriocapillaris blood supply in EOAD patients, and investigated its association with serum AD biomarkers, brain volume, and genetic risk factors. We then evaluated the ability of OCTA parameters to discriminate the EOAD patients and controls. This set of data may indicate the potential of OCTA as a preclinical screening tool for AD.

2 | METHODS

2.1 | Study participants

Participants were selected from the West China Cognitive Impairment Registration study (ChiCTR2000041386), which took place between September 2020 and May 2022 at the Neurology Department of West China Hospital, China. Initially, a discovery cohort of 37 EOAD patients was compared to 31 healthy controls using SS-OCTA, and the results were then replicated in a second confirmatory cohort of 47 EOAD patients compared to 42 healthy controls using SD-OCTA. As part of the study protocol, participants underwent retinal imaging using OCTA, 3T brain magnetic resonance imaging (MRI), and blood draws for AD biomarker analysis (Figure 1). We gathered demographic data, including body mass index, education level, age, and sex.

All participants underwent a Mini-Mental State Examination (MMSE) and Montreal Cognitive Assessment (MoCA) as part of their cognitive evaluations. Furthermore, we meticulously recorded the clinical information of all participants. We ensured that all EOAD patients included in our study met the National Institute on Aging and Alzheimer's Association (NIA-AA) criteria[20] and EOAD diagnostic standards. Furthermore, our study also aligns with the AT(N) framework criteria, revealing significantly elevated levels of amyloid beta (Aβ)42 and phosphorylated tau (p-tau)181 in EOAD patients compared to the healthy controls.[21,22] Inclusion criteria were as follows: (1) clinical signs of dementia or mild cognitive impairment (MCI) with MoCA < 26; (2) typical appearance of the optic nerve head (ONH) and macula; (3) participants were capable of cooperating with the procedures and could tolerate MR imaging, OCTA imaging, and

blood draws. Exclusion criteria were as follows: individuals with (1) a history of other neurological or major psychiatric disorders, such as stroke, brain trauma or tumor, intracranial infection, depression, or schizophrenia; (2) diagnosed with frontotemporal dementia (FTD), dementia with Lewy bodies (DLB), vascular dementia, and other types of dementia rather than AD; (3) a history of ocular disease that could lead to optic fundus diseases such as diabetic retinopathy, severe glaucoma, various eye inflammatory conditions, or eye surgeries (e.g., cataract extraction or laser surgery, severe cataract, glaucoma) within 6 months preceding enrollment; (4) a history of systemic diseases like uncontrolled hypertension or systemic inflammatory disease; (5) a history of any cancer; (6) a history of alcohol or drug abuse. Healthy controls were recruited from local communities, adhering to identical exclusion criteria.

The study was approved by the Biomedical Research Ethics Committee and the Committee on Human Research of West China Hospital, Sichuan University (2020-104). Informed consent was obtained from all participants or their legal guardians.

2.2 | Imaging of retinal microvasculature and choriocapillaris using the SS-OCTA

The SS-OCTA (VG 200; SVision Imaging Limited; version 2.0.106) was used to scan and image the macula and choriocapillaris of all participants. The SS-OCTA, equipped with a swept-source laser with a central wavelength of approximately 1050 nm and a scan rate of 200,000 A-scans per second, captured a high-resolution image (512 × 512 A-scans) of the macula and choriocapillaris (6 × 6 mm) following a three-dimensional protocol. An integrated eye-tracking feature helped reduce projection artifacts while maintaining the true layout.

The SS-OCTA machine's inbuilt algorithm segmented the macula into three plexuses (the superficial vascular plexus, SVP; intermediate capillary plexus, ICP; deep capillary plexus, DCP), and choriocapillaris (Figure S1). The SVP was identified as the microvasculature spanning from the base of the retinal nerve fiber layer (RNFL) to the junction between the inner plexiform layer (IPL) and the inner nuclear layer (INL; Figure S1). The ICP included the microvasculature between the IPL/INL junction and the junction between INL and the outer plexiform layer (OPL). The DCP comprised the microvasculature from the INL/OPL junction to 25 μm below the OPL. The choriocapillaris was defined as the microvasculature from the basal border of the retinal pigment epithelium–Bruch's membrane complex to 20 μm beneath it.

Each image's segmentation was inspected by an independent examiner. The macula images' quality was evaluated both objectively and subjectively, with images with a signal quality below 6 (on a scale of 10) being rejected. Images with artifacts were also discarded. To assess the macular microvasculature and choriocapillaris, we evaluated microvascular perfusion, defined as the length of the perfused microvessels per unit area in square millimeters (mm^2) in the examined region (6 × 6 mm around the fovea).

RESEARCH IN CONTEXT

1. **Systematic review**: We conducted a thorough search of literature databases, including PubMed, to explore studies investigating the connection between retinal microvasculature and Alzheimer's disease (AD) through optical coherence tomography angiography (OCTA). While we identified several relevant studies, there is a limited understanding of retinal vascular metrics variation across various OCTA tools.

2. **Interpretation**: This study examined the relationship between retinal microvascular metrics in AD using the common OCTA tools (swept-source OCTA, and spectral domain OCTA). We showed that early-onset AD (EOAD) patients had significant retinal microvasculature and choriocapillaris changes compared to controls with similar age and sex. We also showed that changes in the choriocapillaris had the highest index to discriminate EOAD from controls.

3. **Future directions**: The potential use of the choriocapillaris using the OCTA deserves further research including mechanisms associated with AD etiology that may be involved. The use of OCTA in identifying persons at risk of AD should be evaluated.

2.3 | Imaging of retinal microvasculature and choriocapillaris using the SD-OCTA

The SD-OCTA (Avanti RTVue, Optovue, Inc.; version 2017.1.0.151) was used for imaging the macula microvasculature and choriocapillaris. With a scan speed of 70,000 A-scans per second and an axial resolution of 5 μm, this device featured a three-dimensional projection artifact removal (3D PAR) to minimize projection artifacts. Implementing a three-dimensional protocol, we obtained a high-resolution image (400 × 400 A-scans) of the macula and choriocapillaris (6 × 6 mm around the fovea).

Inbuilt software in the OCTA tool was used to segment the macula into the superficial vascular complex (SVC) and deep vascular complex (DVC), and choriocapillaris. The segmentation of the SVC and DVC was established at the interface of the inner two thirds and outer one third of the ganglion cell layer and IPL, as illustrated in Figure S1. The choriocapillaris consisted of the microvasculature from the basal border of the retinal pigment epithelium–Bruch's membrane complex to 20 μm beneath it.

Microvascular density was used to evaluate the macular microvasculature and choriocapillaris in the analyzed area (6 × 6 mm around the fovea). Both eyes of all participants were examined on the same day. Measurements that met the criterion of good technical quality,
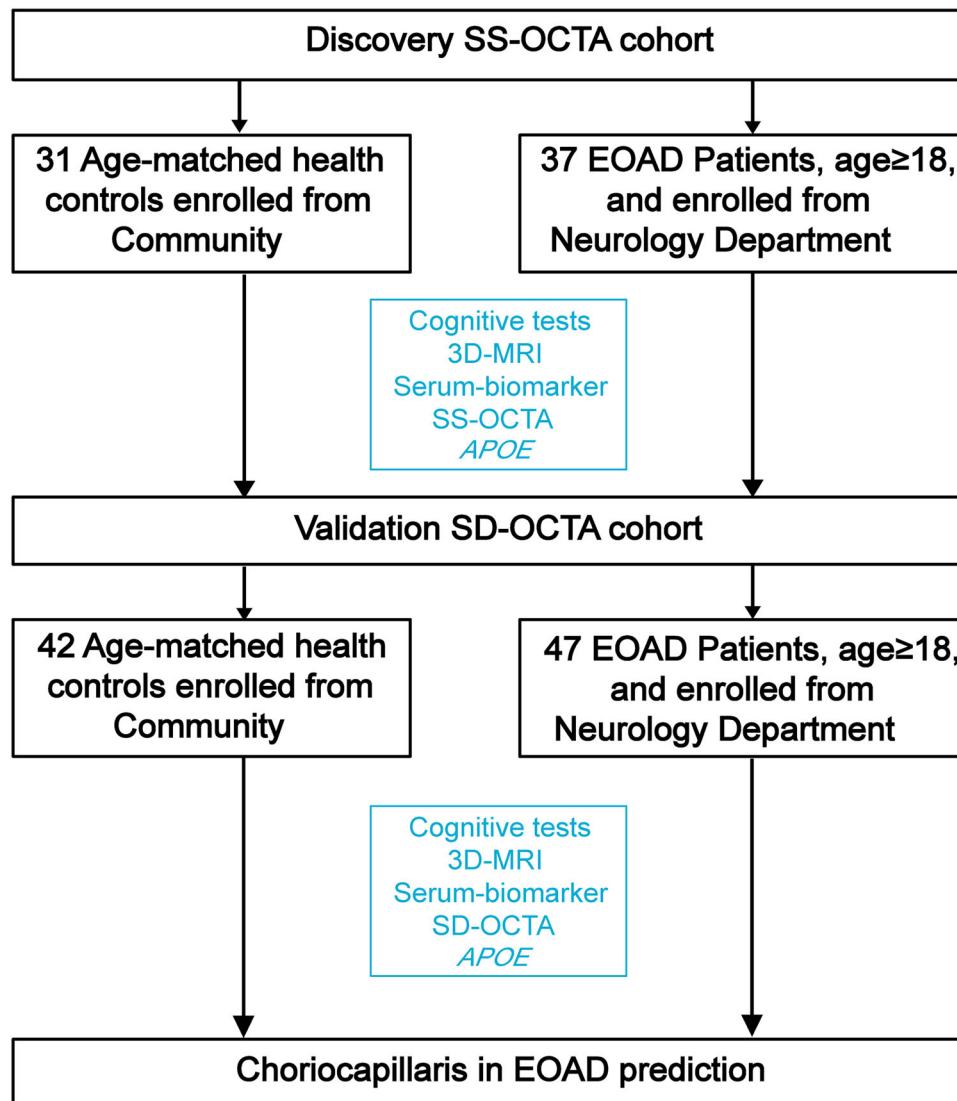
FIGURE 1 Flowchart of study design and patient inclusion. *APOE*, apolipoprotein E; EOAD, early-onset Alzheimer's disease; MRI, magnetic resonance imaging; SD-OCTA, spectral domain optical coherence tomography angiography; SS-OCTA, swept-source optical coherence tomography angiography.

with a signal quality (SQ) of ≥ 7, were considered eligible for further analysis. Angiograms with motion artifacts, such as irregular microvascular patterns or blurred segmentation, were excluded from the analysis.

2.4 | Whole-exome sequencing

Genomic DNA extracted from all EOAD patients underwent whole-exome sequencing (WES) by Annoroad Gene Technology (Beijing). This procedure was conducted on a cBot Cluster Generation System using the Hiseq PE Cluster Kit (Illumina), following the manufacturer's instructions. Valid sequencing data were aligned with the reference human genome (UCSC hg19) using the Burrows–Wheeler Aligner (BWA) software, resulting in BAM-formatted mapping results.[23] Vari-

ant calling and identification of single nucleotide polymorphisms and InDels were performed using Samtools mpileup and bcftools.[24]

2.5 | MRI protocols and imaging analysis

MRI scans were performed on a 3-T MR system (Magnetom Trio, Siemens Medical Systems) in West China Hospital. All patients underwent a standardized protocol, including T1-weighted images, T2-weighted images, fluid-attenuated inversion recovery (FLAIR) images, diffusion-weighted imaging, three-dimensional time-of-flight magnetic resonance angiography (3D-TOF-MRA), and susceptibility-weighted images (SWI). The total brain volume of all participants was measured automatically by the AccuBrain brain structure tool, as reported previously.[19]

2.6 | Blood serum biomarkers

Venous blood was collected in a vacutainer without additives and was then sent to the laboratory within 30 minutes of collection. After centrifugation (845 g for 15 minutes at 4°C), serum was collected and immediately frozen at −80°C until further use. Serum Aβ40, Aβ42, and total tau (t-tau) were analyzed using Quanterix Simoa Human Neurology 3-Plex E essays (Cat No. 101995), and p-tau181 was measured using Quanterix Simoa p-tau 181 Advantage V2 Kits (Cat No. 103714). Assays were performed using a Quanterix single-molecule array (Simoa) SR-X analyzer platform (Quanterix), as guided by the manufacturer's manual, as previously reported.[25] All samples were analyzed concurrently to avoid the batch effect.

2.7 | Statistical analyses

The Shapiro–Wilk test was used to determine the normality of the data. Continuous variables with normal distributions were expressed as the mean ± standard deviations, while skewed distributions were presented as medians and interquartile ranges. All statistical analyses were performed in R Core Team (2017) unless noted otherwise. The Statistical R software version 3.4.1 (http://www.R-project.org) was used to analyze the associations among OCTA parameters, blood serum biomarkers, and neuroimaging parameters. Generalized estimating equations (GEE) were used to compare the OCTA parameters between EOAD patients and controls, adjusting for risk factors (age, sex, hypertension, and education) and intereye dependencies. A multiple linear regression model with GEE was used to assess the associations among SS-OCTA parameters, blood serum biomarkers, and neuroimaging parameters, adjusting for risk factors (age, sex, hypertension, and education) and intereye dependencies. The area under the receiver operating characteristic (AUROC) was calculated to determine the diagnostic capability of the OCTA parameters in EOAD patients versus controls; an AUROC of 1.0 represents perfect discrimination, whereas 0.5 indicates random discrimination. P values < 0.05 were considered statistically significant.

3 | RESULTS

Our data analysis included 84 patients with EOAD diagnosis in total (mean age, 61.1 ± 6.5 years) and 73 healthy controls (HCs; mean age, 60.5 ± 7.1 years; P = 0.621; Table S1 in supporting information). No significant differences were observed in age, sex, hypertension, diabetes, dyslipidemia, and education. EOAD patients exhibited significantly reduced MoCA scores (8.0, interquartile range [IQR]: 6.0–14.2; P < 0.001) relative to controls. Furthermore, EOAD patients presented a general reduction in total brain volume as well as specific brain lobes (1077 vs. 1145 cm^3; Table S1). Notably, the EOAD group displayed significantly elevated levels of Aβ40 (96.5, IQR: 41.4–133.2 pg/mL, P < 0.001), Aβ42 (8.41, IQR: 6.18–12.91 pg/mL, P < 0.001), Aβ42/40 (0.074, IQR: 0.060–0.103, P = 0.001), and p-tau181 (1.89, IQR: 1.18–3.03 pg/mL, P < 0.001; Table S1, Figure S2A in supporting information),

consistent with AD diagnosis. In this study, we used a discovery cohort of SS-OCTA to explore the predictive capabilities of the choriocapillaris in EOAD. Subsequently, we validated this discovery in the SD-OCTA cohort. In both cohorts, the baseline characteristics were comparable, such as age, sex, and education history (Tables 1 and 2).

3.1 | SD-OCTA and SS-OCTA showed choriocapillaris as the best diagnostic indicator for EOAD

Within the SS-OCTA cohort, EOAD patients showed a significant reduction in the density of SVP (1.20 ± 0.20 mm^2; P = 0.002), ICP (0.91 ± 0.20 mm^2; P = 0.001), DCP (0.72 ± 0.16 mm^2; P < 0.001), and choriocapillaris (2.53 ± 0.24 mm^2; P < 0.001) compared to the control group (Table 1 and Figure 2A). Similarly, in the SD-OCTA cohort, EOAD patients exhibited a significant decrease in the density of SVC (49.23 ± 3.40%; P = 0.004), DVC (48.73 ± 4.66%; P < 0.001), and choriocapillaris (65.98 ± 3.25%; P < 0.001) compared to the control subjects (Table 2 and Figure 3A).

In the SS-OCTA cohort, choriocapillaris perfusion demonstrated the highest area under the curve (AUC = 0.913, 95% confidence interval[CI]: 0.808–0.909, sensitivity = 82%, specificity = 100%, positive predictive value [PPV] = 0.95, 95% CI: 0.87–0.99; negative predictive value [NPV] = 0.79, 95% CI: 0.68–0.87; P < 0.001; Figure 2B), making it the most effective among all SS-OCTA parameters for detecting microvascular changes in EOAD and healthy controls. Similarly, in the SD-OCTA cohort, choriocapillaris exhibited the greatest AUC (AUC = 0.991, 95% CI: 0.692–0.816, sensitivity = 69%, specificity = 94%, PPV = 1.00, 95% CI: 0.96–1.00; NPV = 0.92, 95% CI: 0.83–0.97; P < 0.001; Figure 3B), outperforming other SD-OCTA parameters in identifying microvascular changes in EOAD and controls. Among the serum biomarkers, EOAD patients showed significantly elevated levels of Aβ40 (91.1, IQR = 55.4–106.4 pg/mL, P = 0.031), Aβ42 (8.25, IQR = 6.36–9.55 pg/mL, P = 0.026) and p-tau181 (1.51, IQR = 0.89–2.55 pg/mL, P < 0.001) compared to the control group in the SS-OCTA cohort (Table 1 and Figure 2C).Similar results were also observed in the SD-OCTA cohort (Table 2 and Figure 3C). When combining the SS-OCTA and SD-OCTA cohorts, Aβ42 and p-tau181 showed improved performance (AUC = 0.844, 95% CI: 0.799–0.889, sensitivity = 72%, specificity = 86%, PPV = 0.82, 95% CI: 0.74–0.89; NPV = 0.77, 95% CI: 0.70–0.83; and AUC = 0.926, 95% CI: 0.894–0.958, sensitivity = 97%, specificity = 81%, PPV = 0.97, 95% CI: 0.92–0.99; NPV = 0.81, 95% CI: 0.73–0.86, respectively; Figure S2B). Similar results can be observed in the two separate cohorts (Figures 2D and 3D).

3.2 | Parameters of SS-OCTA correlated with Aβ and p-tau181 levels and parietal lobe volume

We investigated the correlations among OCTA parameters, blood biomarkers, and brain volume in EOAD patients. It was found that SS-OCTA parameters had a stronger correlation with blood biomark-

TABLE 1 Demographics and clinical information in SS-OCTA cohort.

SS-OCTA	Controls (n = 31)	EOAD (n = 37)	P value
Age, years	64.0 ± 5.8	62.2 ± 5.9	0.191
Female, n (%)	19 (61.3%)	15 (40.5%)	0.144
Hypertension, n (%)	11 (35.5%)	13 (35.1%)	1.000
Diabetes, n (%)	7 (22.6%)	6 (16.2%)	0.722
Dyslipidemia, n (%)	3 (9.7%)	6 (16.7%)	0.633
Education, years	9.0 (6.0–12.0)	6.0 (6.0–9.0)	0.063
MoCA Score	28.0 (26.0–29.0)	10.0 (6.0–15.0)	<0.001
Total volume + CSF, cm^3	1443 (1368–1593)	1441 (1311–1524)	0.040
Total volume, cm^3	1136 (1071–1186)	1085 (990–1129)	<0.001
Hippocampus, cm^3	6.9 (6.7–7.2)	5.3 (4.5–6.3)	<0.001
Frontal lobe, cm^3	151.6 (147.2–159.6)	145.4 (131.6–157.9)	0.014
Occipital lobe, cm^3	68 (66–72)	66 (60–70)	0.027
Temporal lobe, cm^3	103.5 (99.0–112.9)	92.4 (85.2–98.1)	<0.001
Parietal lobe, cm^3	73.1 (71.0–76.1)	70.7 (62.1–75.0)	0.040
Aβ40, pg/mL	52.6 (41.8–82.0)	91.1 (55.4–106.4)	0.031
Aβ42, pg/mL	4.52 (1.28–5.73)	8.25 (6.36–9.55)	0.026
Aβ42/40	0.070 (0.040–0.094)	0.080 (0.070–0.110)	0.057
Tau, pg/mL	0.70 (0.43–0.82)	0.64 (0.42–0.94)	0.763
p-tau181, pg/mL	0.30 (0.20–0.61)	1.51 (0.89–2.55)	<0.001
SVP, mm^2	1.28 ± 0.08	1.20 ± 0.20	0.002
ICP, mm^2	1.00 ± 0.07	0.91 ± 0.20	0.001
DCP, mm^2	0.86 ± 0.06	0.72 ± 0.16	<0.001
Choriocapillaris, mm^2	2.83 ± 0.08	2.53 ± 0.24	<0.001

Note: Data were expressed as mean (standard deviation) or frequency (%) as appropriate.
Abbreviations: Aβ, amyloid beta; CSF, cerebrospinal fluid; DCP, deep capillary plexus; EOAD, early-onset Alzheimer's disease; HC, healthy controls; ICP, intermediate capillary plexus; IOP, intraocular pressure, measured in millimeters per mercury (mmHg); MMSE, Mini-Mental State Examination; MoCA, Montreal Cognitive Assessment; p-tau, phosphorylated tau; SS-OCTA, swept-source optical coherence tomography angiography; SVP, superficial vascular plexus.

ers compared to SD-OCTA parameters (Tables S2–S4 in supporting information and Figure 2E). In the SS-OCTA group, a decreased density of the choriocapillaris was correlated with increased levels of Aβ42 (P = 0.004), Aβ42/40 (P < 0.001), and p-tau181 (P = 0.032). It also displayed a linear correlation with decreased levels of Aβ40 (P = 0.002; Table 3 and Figure 2E). Moreover, except choriocapillaris (P = 0.389), the parameters of SVP (P = 0.017), ICP (P = 0.005), and DCP (P = 0.0147) were linearly associated with the volume of the parietal lobe (Table S3, Figure 2F).

3.3 | Apolipoprotein E ε4(+) patients exhibited sparser choriocapillaris and elevated total tau levels in the SS-OCTA cohort

Comprehensive exon genotyping was carried out in all EOAD patients to examine the variations in OCTA parameters among different genotypes. Among the EOAD patients, we identified five individuals with pathogenic mutations in *APP*, *PSEN1*, or *PSEN2*, and seven individuals likely to carry risk mutations in the *PRNP*, *SORL1*, *C9ORF72*, or *FUS*

genes (Table S5 in supporting information). We categorized cohorts based on the likelihood of carrying a pathogenic gene; however, no significant results were observed (Table S6 in supporting information).

Among the patients, 53 tested negative for apolipoprotein E (*APOE*) ε4, while 31 tested positive. As presented in Table 4 and Figure 4, the baseline characteristics were largely similar between *APOE* carriers (*APOE* ε4(+)) and *APOE* non-carriers (*APOE* ε4(–)), except for a higher prevalence of hypertension (32.3%, P = 0.042), increased serum tau levels (0.85 pg/mL, P = 0.045), and reduced hippocampus volume (5.2 cm^3, P = 0.002) in *APOE* ε4(+) patients. Additionally, *APOE* ε4(+) patients in the SS-OCTA cohort exhibited lower SVP (1.15 ± 0.22 mm^2, P = 0.038), DCP (0.68 ± 0.17 mm^2, P = 0.026), and choriocapillaris density (2.42 ± 0.26 mm^2, P < 0.001), a trend not observed in the SD-OCTA cohort (Figure S3 in supporting information).

When regressing *APOE* ε4, choriocapillaris, and Aβ42 levels together, mediation analysis revealed that sparser choriocapillaris continued to be associated with the Aβ42 level after controlling for *APOE* ε4 (P = 0.0004). The direct effect (DE) was 17.260 (95% CI −37.426 to 2.74, P = 0.0876), and −70.70% of the mediation contributed to larger choriocapillaris (P = 0.7792; Figure S4 in supporting

TABLE 2 Demographics and clinical information in SD-OCTA cohort.

SD-OCTA	Controls (n = 42)	EOAD (n = 47)	P value
Age, years	58.0 ± 6.9	60.2 ± 6.9	0.126
Female, n (%)	22 (52.4%)	23 (48.9%)	0.910
Hypertension, n (%)	2 (4.8%)	3 (6.4%)	1.000
Diabetes, n (%)	0 (0.0%)	0 (0.0%)	0.596
Dyslipidemia, n (%)	3 (7.1%)	1 (2.1%)	0.530
Education, years	9.0 (6.0–12.0)	9.0 (7.5–12.0)	0.809
MoCA Score	28.0 (26.0–29.0)	8.0 (5.0–13.0)	<0.001
Total volume + CSF, cm^3	1482 (1371–1597)	1435 (1297–1509)	0.033
Total volume, cm^3	1149 (1060–1195)	1075 (972–1111)	0.002
Hippocampus, cm^3	6.8 (6.3–6.9)	5.7 (5.1–6.4)	<0.001
Frontal lobe, cm^3	157.7 (146.9–168.9)	147.7 (134.9–157.9)	0.002
Occipital lobe, cm^3	68 (61–74)	65 (56–70)	0.247
Temporal lobe, cm^3	101.1 (94.8–108.3)	90.7 (83.6–97.8)	<0.001
Parietal lobe, cm^3	77.4 (74.4–83.9)	67.0 (59.9–72.6)	<0.001
Aβ40, pg/mL	49.2 (23.1–68.0)	108.2 (28.4–140.8)	<0.001
Aβ42, pg/mL	2.09 (0.61–4.40)	8.59 (6.07–13.66)	<0.001
Aβ42/40	0.049 (0.030–0.076)	0.072 (0.056–0.092)	0.011
Tau, pg/mL	0.81 (0.54–1.06)	45; 0.72 (0.53–1.17)	0.168
p-tau181, pg/mL	0.36 (0.20–0.52)	40; 2.11 (1.52–3.31)	<0.001
SVC, %	50.73 ± 3.13	49.23 ± 3.40	0.004
DVC, %	53.99 ± 4.15	48.73 ± 4.66	<0.001
Choriocapillaris, %	74.07 ± 2.15	65.98 ± 3.25	<0.001

Note: Data were expressed as mean (standard deviation) or frequency (%) as appropriate.

Abbreviations: Aβ, amyloid beta; CSF, cerebrospinal fluid; DVC, deep vascular complex; EOAD, early-onset Alzheimer's disease; MoCA, Montreal Cognitive Assessment; p-tau, phosphorylated tau; SD-OCTA, spectral domain optical coherence tomography angiography; SVC, superficial vascular complex.

information). This suggested that choriocapillaris did not significantly mediate the effect of *APOE ε4* with Aβ42 levels.

4 | DISCUSSION

The discovery of novel and preferably non-invasive biomarkers to predict AD is of paramount importance.[26] Presently, the diagnosis of preclinical AD relies on Aβ positron emission tomography (PET), cerebrospinal fluid (CSF), or blood Aβ or tau levels.[27] Although effective, these measurements are invasive, expensive, and heavily equipment dependent, making them challenging to apply worldwide, particularly in low- and middle-income countries. The current study identified a potential alternative by using OCTA. We found that impairments in the choriocapillaris (a layer of capillaries in the eye) detected by both SS-OCTA and SD-OCTA were highly discriminatory in diagnosing EOAD. The choriocapillaris in SS-OCTA linearly correlated with serum Aβ, indicating that changes in the blood flow of the eye may relate to Aβ pathology. Therefore, OCTA might serve as a non-invasive, cost-effective early screening tool for AD in the preclinical stage, particularly beneficial for resource-limited settings.

Vascular dysfunction may precede the traditional pathological hallmarks of AD.[28–31] For instance, microvasculature degeneration, including the number of vessel segments and vessel-to-vessel junctions, appeared as early as 3 months of age, while the hippocampal Aβ plaques were only observed at 6 months of age in a triple-transgenic AD mouse model (3xTg AD mice).[28] Given the shared pathophysiology between the retina and the brain, it is proposed that changes in the retinal microvasculature mirror those occurring in the cerebral microvasculature.[32–35] In line with this, we found a linear correlation between the choriocapillaris and serum Aβ levels, indicating that measuring these retinal changes may have potential as an early screening tool for the preclinical stage of AD. This finding also links the degeneration of fundus microvasculature with Aβ levels during AD progression, a conclusion that aligns with recent studies.[14,36]

Although blood Aβ levels have been evaluated as a possible diagnostic marker for AD, the results were inconsistent. Several systematic reviews have indicated that levels of Aβ42 and Aβ42/40 in the blood of AD patients are elevated while others reported the opposite results.[37–40] We here found a significant increase in serum Aβ42 levels, as shown in Table S1. More importantly, our study identified a significant increase in p-tau181 levels in EOAD and
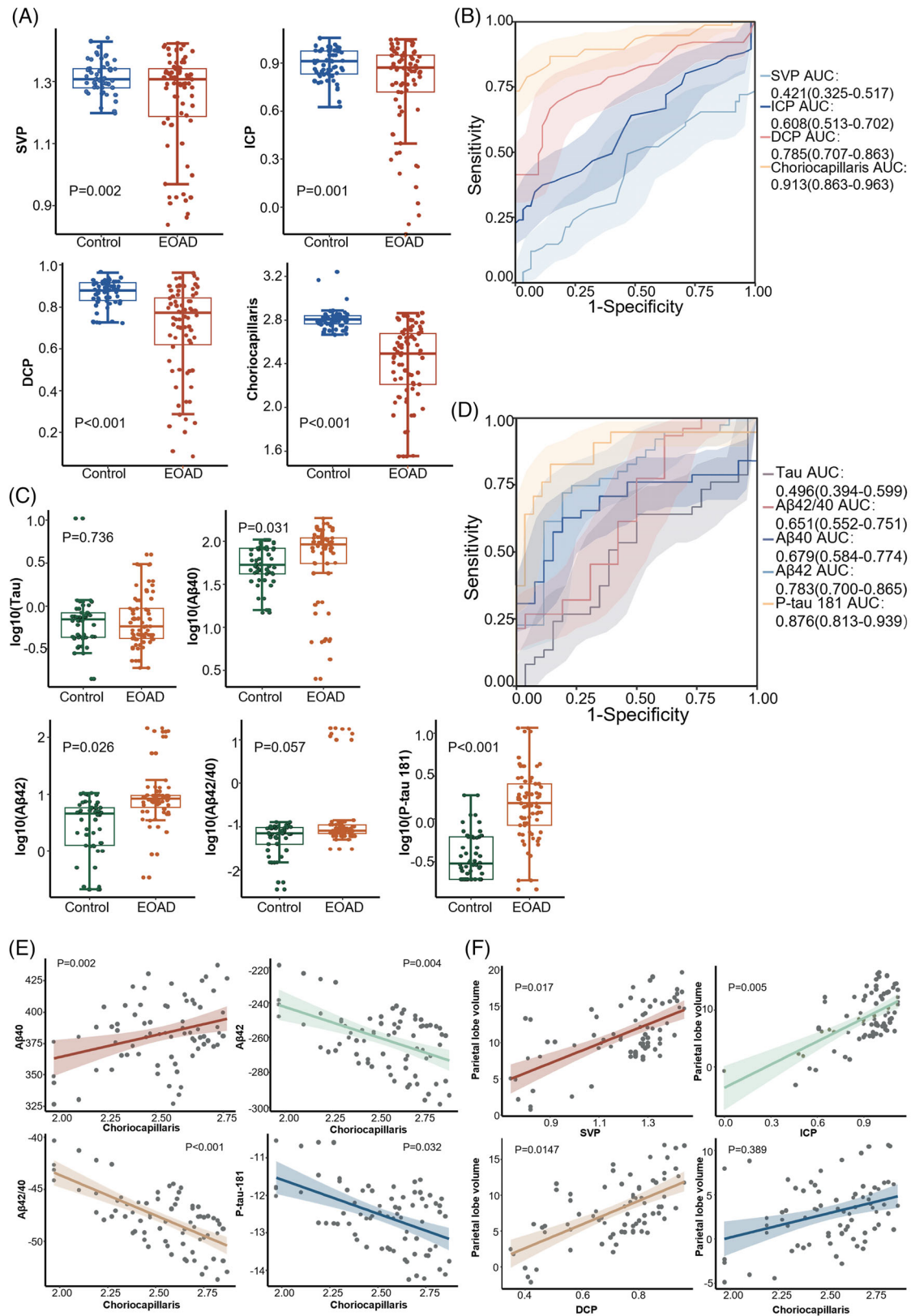
FIGURE 2 The choriocapillaris and serum biomarkers in SS-OCTA cohort. A, Comparison of SS-OCTA parameters between the control and EOAD groups (data source: Table 1); (B) ROC analysis of SS-OCTA parameters (data source: Table 1); (C) comparison of serum biomarkers between the control and EOAD groups (data source: Table 1); (D) ROC analysis of SS-OCTA parameters (data source: Table 1); (E) linear correlation between choriocapillaris and serum biomarkers in EOAD (data source: Table 3); (F) linear correlation between choriocapillaris and parietal lobe volume in EOAD (data source: Table S3). DCP, deep capillary plexus; EOAD, early-onset Alzheimer's disease; ICP, intermediate capillary plexus; ROC, receiver operating characteristic; SS-OCTA, swept-source optical coherence tomography angiography; SVP, superficial vascular plexus.
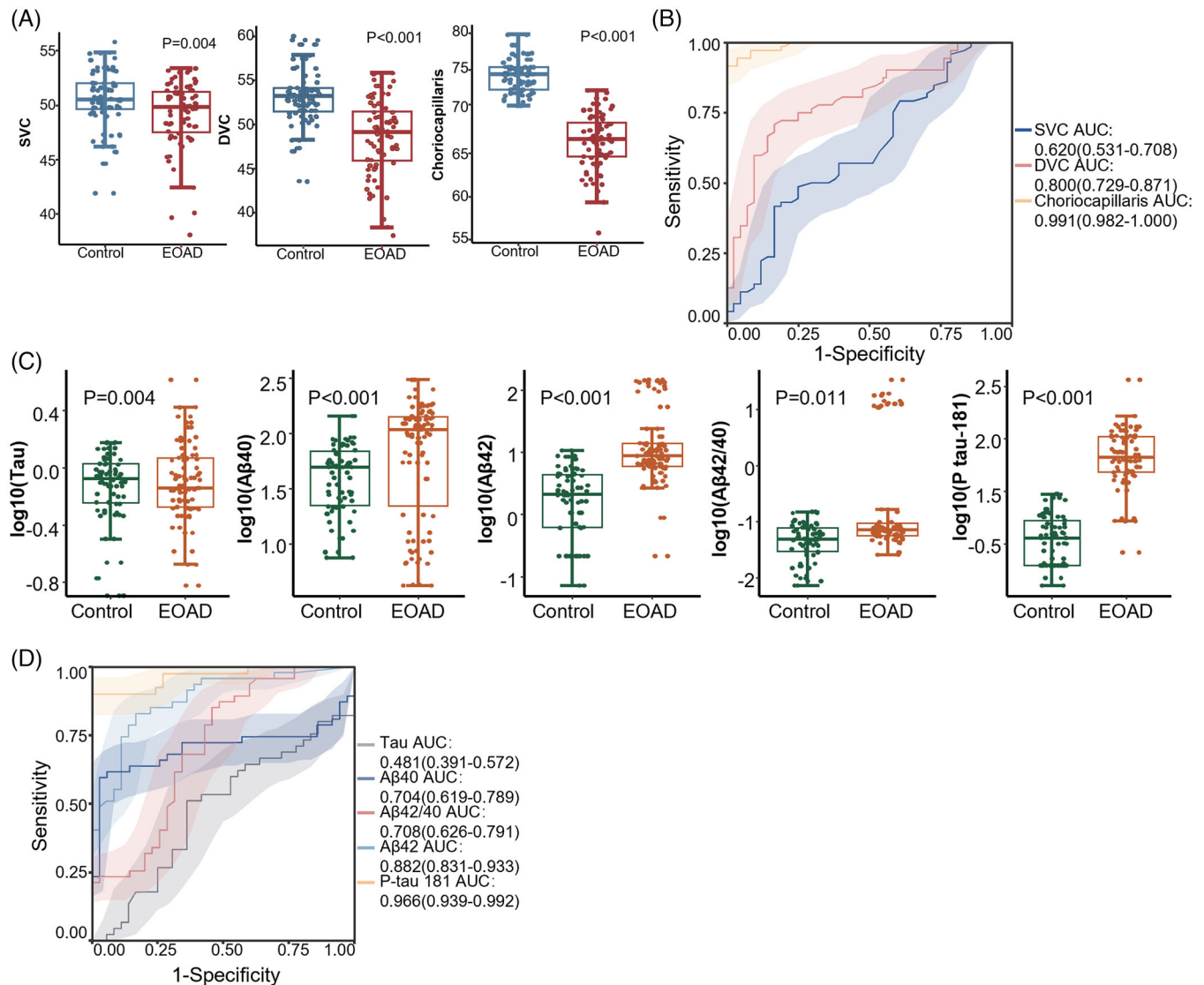
FIGURE 3 The choriocapillaris and serum biomarkers in SD-OCTA cohort. A, Comparison of SD-OCTA parameters between the control and EOAD groups (data source: Table 2); (B) ROC analysis of SD-OCTA parameters (data source: Table 2); (C) comparison of serum biomarkers between the control and EOAD groups (data source: Table 2); (D) ROC analysis of SD-OCTA parameters (data source: Table 2). DVC, deep vascular complex; EOAD, early-onset Alzheimer's disease; ICP, intermediate capillary plexus; ROC, receiver operating characteristic; SD-OCTA, spectral domain optical coherence tomography angiography; SVC, superficial vascular complex.

correlated with microvascular impairment in the choriocapillaris in these patients.[22,41–43]

While it was widely acknowledged that microvascular dysfunction played a significant role in the pathogenesis of AD, a key challenge lay in the limited observability and quantifiability of microvasculature.[44] Interestingly, the cerebral and retinal vasculature exhibit structural similarities and share common hemodynamic properties.[32,45] Recent research has further suggested that the functionality of retinal microvessels is linked to that of cerebral microcirculation, offering a potential avenue for the early detection of brain microvascular dysfunction.[33,34] Choroidal vasculature, which receives its circulation from the ciliary arteries of the ophthalmic artery, compensates for retinal microvascular dropout (especially in the DCP) during hypoxia, conditions of reduced oxygen supply.[46,47] Given the close relationship

between choriocapillaris and retinal microvasculature, the choriocapillaris could be considered more sensitive to ischemic changes that occur in the retina, such as DCP (Figure S5 in supporting information). This highlights its potential as a valuable target for observation and evaluation in eye health and diseases, such as in the case of EOAD. Recent reports also suggested that thinning of the choroid in AD points to an abnormal choroidal blood supply associated with vasoregression or pathological events triggered by Aβ deposition in the brain.[13,48] The choroidal microvasculature has received much less attention than the total choroidal thickness in previous studies. A more comprehensive understanding of the choroidal microvasculature is necessary given its sensitivity to reduced oxygen supply.

The choroid consists of four vascular layers, and this study focused on the choriocapillaris because it is sensitive to ischemic changes

TABLE 3 Correlation between serum biomarkers and SS-OCTA parameters.

Variable	SVP			ICP			DCP			Choriocapillaris		
	β Coefficient	SE	P value	β Coefficient	SE	P value	β Coefficient	SE	P value	β Coefficient	SE	P value
Tau	−0.996	0.510	0.055	−1.434	0.486	0.004	−1.496	0.628	0.020	−0.120	0.450	0.790
p-tau181	−5.897	1.307	<0.001	−7.003	1.197	<0.001	−8.468	1.550	<0.001	−2.712	1.237	0.032
Aβ40	61.309	25.264	0.018	63.297	24.774	0.013	76.568	31.524	0.018	67.337	21.091	0.002
Aβ42	−100.809	19.105	<0.001	−111.675	17.764	<0.001	−137.139	22.903	<0.001	−54.889	18.307	0.004
Aβ42/40	−14.020	2.666	<0.001	−13.038	2.683	<0.001	−18.223	3.269	<0.001	−10.887	2.373	<0.001

Abbreviations: Aβ, amyloid beta; DCP, deep capillary plexus; ICP, intermediate capillary plexus; p-tau, phosphorylated tau; SS-OCTA, swept-source optical coherence tomography angiography; SVP, superficial vascular plexus.

TABLE 4 Baseline features between *APOE* ε4 (+) and *APOE* ε4 (−) EOAD patients.

APOE	APOE ε4 (−) (n = 53)	APOE ε4 (+) (n = 31)	P value
Age, years	60.4 ± 5.8	62.4 ± 7.6	0.186
Female, *n* (%)	26 (50.0%)	11 (35.5%)	0.289
Hypertension, *n* (%)	6 (11.5%)	10 (32.3%)	0.042
Diabetes, *n* (%)	4 (7.7%)	2 (6.5%)	1.000
Dyslipidemia, *n* (%)	4/51 (7.8%)	3 (9.7%)	1.000
Education, years	9.0 (6.0–12.0)	9.0 (6.0–10.5)	0.963
MoCA score	9.0 (6.0–15.0)	8.0 (5.0–12.0)	0.180
Total volume + CSF, cm^3	1463 (1327–1524)	1370 (1271–1466)	0.111
Total volume, cm^3	1085 (982–1111)	1009 (964–1119)	0.167
Hippocampus, cm^3	6.2 (5.2–6.5)	5.2 (4.2–5.6)	0.002
Frontal lobe, cm^3	145.6 (134.7–158.9)	146.0 (131.6–157.1)	0.729
Occipital lobe, cm^3	66 (56–71)	64 (59–68)	0.738
Temporal lobe, cm^3	93.9 (84.2–98.1)	89.8 (82.0–95.4)	0.337
Parietal lobe, cm^3	69.7 (61.0–72.9)	65.6 (61.4–73.7)	0.927
Aβ40, pg/mL	102.9 (19.2–135.0)	87.0 (54.2–108.9)	0.580
Aβ42, pg/mL	8.59 (5.84–13.13)	7.83 (6.38–10.94)	0.448
Aβ42/40	0.072 (0.060–0.090)	0.080 (0.069–0.120)	0.543
Tau, pg/mL	0.71 (0.47–0.90)	0.85 (0.46–1.54)	0.045
p-tau181, pg/mL	1.92 (1.08–3.23)	1.79 (1.29–2.68)	0.322
SS-OCTA cohort			
SVP, mm^2	1.24 ± 0.16	1.15 ± 0.22	0.038
ICP, mm^2	0.94 ± 0.21	0.86 ± 0.18	0.077
DCP, mm^2	0.76 ± 0.14	0.68 ± 0.17	0.026
Choriocapillaris, mm^2	2.63 ± 0.17	2.42 ± 0.26	<0.001
SD-OCTA cohort			
SVC, %	49.65 ± 3.07	48.06 ± 4.05	0.081
DVC, %	48.93 ± 4.39	48.19 ± 5.43	0.557
Choriocapillaris, %	65.55 ± 3.12	67.19 ± 3.39	0.058

Note: Data were expressed as mean (standard deviation) or frequency (%) as appropriate.
Abbreviations: Aβ, amyloid beta; *APOE*, apolipoprotein E; CSF, cerebrospinal fluid; DCP, deep capillary plexus; DVC, deep vascular complex; EOAD, early-onset Alzheimer's disease; ICP, intermediate capillary plexus; MoCA, Montreal Cognitive Assessment; p-tau, phosphorylated tau; SD-OCTA, spectral domain optical coherence tomography angiography; SS-OCTA, swept-source optical coherence tomography angiography; SVC, superficial vascular complex; SVP, superficial vascular plexus.
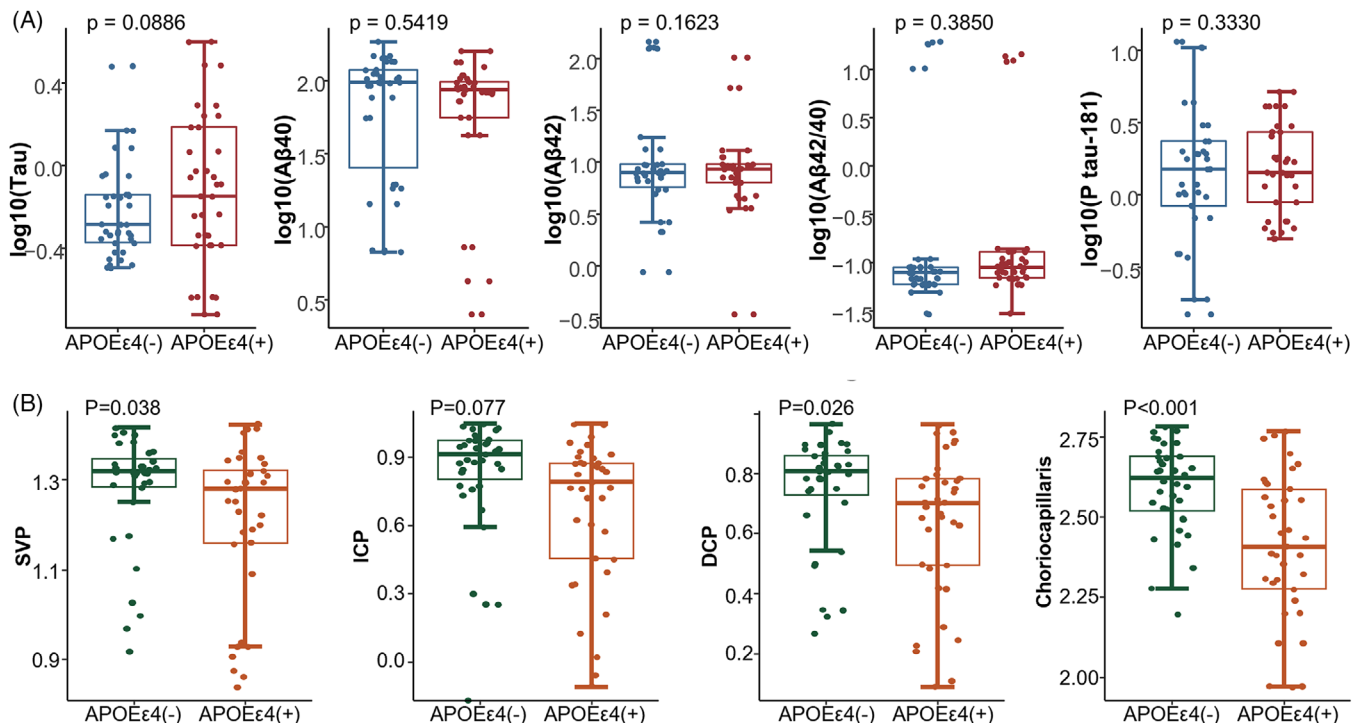
FIGURE 4 The choriocapillaris and serum biomarkers according to *APOE* in SS-OCTA cohort. A, Comparison of serum biomarkers according to *APOE* in EOAD (data source: Table 4); (B) comparison of SS-OCTA parameters according to *APOE* in EOAD (data source: Table 4). *APOE*, apolipoprotein E; DCP, deep capillary plexus; ICP, intermediate capillary plexus; SS-OCTA, swept-source optical coherence tomography angiography; SVP, superficial vascular plexus.

that occur in the retina and can be assessed consistently by both the SS-OCTA and the SD-OCTA methods. Moreover, a wide range of retinal microvascular and choriocapillaris changes in AD patients such as lower densities, sparser vasculature, increased tortuosity, and lower fractal dimensions have been shown in OCTA studies.[8,49–53] Here we showed that EOAD patients had lower retinal microvascular and choriocapillaris densities and sparser retinal microvascular and choriocapillaris compared to controls. These findings are in line with previous OCTA analyses. It is noteworthy that we found that the choriocapillaris were most sensitive to microvascular damage in EOAD, indicating that choriocapillaris may accurately discriminate against EOAD compared to controls. Additionally, EOAD patients show widespread cortical atrophy, particularly in the parietal cortex, assessed by cerebral imaging. We found that EOAD patients had lower parietal lobe volumes compared to controls, which is congruent with previous reports.[54,55] We also found that sparser retinal microvasculature in EOAD patients correlated with reduced parietal lobe volume. This may suggest a possible link between cerebral structural volume and retinal microvasculature where cerebral neurodegeneration may be related to microvascular impairment in the retina of EOAD patients.

Both SS-OCTA and SD-OCTA cohorts indicated that the choriocapillaris displayed the most substantial discriminative power in identifying EOAD patients from controls. Moreover, the choriocapillaris metrics obtained from the SS-OCTA demonstrated significant correlations with blood-based parameters in our study. While both

OCTA tools use the Fourier domain detection technique, the SS-OCTA has a faster scanning speed, permitting denser scan patterns and larger scans compared to the SD-OCTA.[56] Additionally, the SS-OCTA operates at a longer wavelength, facilitating enhanced light penetration through the retinal pigment epithelium. These advantages enable the SS-OCTA to overcome the RPE barrier, leading to improved choroid detection. Nevertheless, both machines demonstrated that the choriocapillaris possessed the highest discriminative power (AUROC) for EOAD patients. SD-OCTA is more accessible in China due to its cost effectiveness even in remote regions, making it suitable for the early screening of choriocapillaris abnormalities.

The *APOE* ε4 genotype is recognized as a significant genetic risk factor for sporadic AD. Existing literature has established that *APOE* ε4 influences microvascular density and function.[57,58] Our SS-OCTA analysis revealed a sparser SVP, DCP, and choriocapillaris in *APOE* ε4 carriers compared to non-carriers. This aligns with the previous findings,[7] which reported reduced retinal microvascular density in *APOE* ε4 carriers versus non-carriers. A noteworthy correlation was found between the choriocapillaris measurements obtained from SS-OCTA and the Aβ isoforms and p-tau181 levels. This correlation, coupled with the observed reduction in choriocapillaris among *APOE* ε4 carriers, implies that a reduced blood supply of choriocapillaris could potentially serve as an early predictive marker for dementia. Our findings raise the possibility that microvascular changes within the choriocapillaris might precede neuronal changes in EOAD patients with *APOE* ε4. This hypothesis is in harmony with previous OCTA

studies[59–61] and autopsy reports on late-onset dementia,[62] which suggest the temporal precedence of vascular changes over neuronal alterations. Considering that the mediating effect of the choriocapillaris in the association between *APOE* ε4 and Aβ42 levels was not positive, further investigation is required to confirm this potentially pivotal timeline of pathological events in AD progression.

One of the principal strengths of our study lies in the in vivo imaging and quantitative measurement of three microvascular plexuses and the choriocapillaris. This was achieved through the use of two types of OCTA devices—SS-OCTA and SD-OCTA—offering a degree of cross-validation. SS-OCTA, with its longer wavelength, provided a more detailed and contrasting view of the retina and choroid compared to SD-OCTA. This in vivo quantification of the microvascular plexuses and choriocapillaris holds the potential for tracking EOAD progression and assessing the efficacy of proposed treatments. Moreover, our study extended the investigation beyond the central area of the retina, encompassing a larger area in line with suggestions that most dementia-related pathologies localize in the peripheral part of the retina.[36] Furthermore, the reduction of projection artifacts was more effective in the 6 mm region around the fovea than in the standard 3 mm region.

Nonetheless, our study also has limitations. As an observational, cross-sectional, non-interventional study, we were unable to ascertain causal mechanisms. To address this limitation, we have initiated a longitudinal study involving annual follow-ups with our patients (ChiCTR2000041386). Additionally, our modest sample size is a recognized limitation, with larger cohorts needed to replicate and validate our findings. Moreover, the current study design did not include provisions for multiple group comparisons. However, by comparing various groups such as MCI, EOAD, late-onset AD (LOAD), and non-AD dementia, we may achieve a more comprehensive understanding of the specificity of our findings across different degrees and subtypes of dementia. Furthermore, in the original design, we tested the *APOE* status only in the EOAD cohort. In future follow-up longitudinal studies, we will test the *APOE* status in controls to investigate if it affects the ability of OCTA parameters to predict the conversion from cognitive normal to MCI.

The results from this comprehensive study highlight choriocapillaris impairment, exhibiting a linear correlation with serum Aβ levels, as the most sensitive discriminative marker between EOAD individuals and controls. Our findings also propose that the degeneration of choroid microvasculature may evolve in concert with the classical AD biomarkers, thereby positioning choroid microvasculature as a potential preclinical imaging marker for AD screening with great accessibility.

AUTHOR CONTRIBUTIONS

ACKNOWLEDGMENTS

CONFLICT OF INTEREST STATEMENT

The sponsor had no role in the study design, data collection, data analysis, data interpretation, or writing of the report. All authors had full access to all the study data. The corresponding author had final responsibility for the decision to submit the manuscript for publication. Author disclosures are available in the supporting information.

CONSENT STATEMENT

Informed consent was obtained from participants or their guardians.

REFERENCES

1. Tolar M, Abushakra S, Sabbagh M. The path forward in Alzheimer's disease therapeutics: reevaluating the amyloid cascade hypothesis. *Alzheimers Dement.* 2020;16(11):1553-1560. doi:10.1016/j.jalz.2019.09.075

2. Hussong SA, Banh AQ, Van Skike CE, et al. Soluble pathogenic tau enters brain vascular endothelial cells and drives cellular senescence and brain microvascular dysfunction in a mouse model of tauopathy. *Nat Commun.* 2023;14(1):2367. doi:10.1038/s41467-023-37840-y

3. Drachman DA, Smith TW, Alkamachi B, Kane K. Microvascular changes in Down syndrome with Alzheimer's-type pathology: insights into a potential vascular mechanism for Down syndrome and Alzheimer's disease. *Alzheimers Dement.* 2017;13(12):1389-1396. doi:10.1016/j.jalz.2017.05.003

4. Cheung CY, Ong YT, Ikram MK, et al. Microvascular network alterations in the retina of patients with Alzheimer's disease. *Alzheimers Dement.* 2014;10(2):135-142. doi:10.1016/j.jalz.2013.06.009

5. Felsky D, Roostaei T, Nho K, et al. Neuropathological correlates and genetic architecture of microglial activation in elderly human brain. *Nat Commun.* 2019;10(1):409. doi:10.1038/s41467-018-08279-3

6. Broce IJ, Tan CH, Fan CC, et al. Dissecting the genetic relationship between cardiovascular risk factors and Alzheimer's disease. *Acta Neuropathol.* 2019;137(2):209-226. doi:10.1007/s00401-018-1928-6

7. Xiong H, Tang F, Guo Y, Xu R, Lei P. Neural circuit changes in neurological disorders: evidence from in vivo two-photon imaging. *Ageing Res Rev.* 2023;87:101933. doi:10.1016/j.arr.2023.101933

8. Snyder PJ, Alber J, Alt C, et al. Retinal imaging in Alzheimer's and neurodegenerative diseases. *Alzheimers Dement.* 2021;17(1):103-111. doi:10.1002/alz.12179

9. Zlokovic BV. Neurovascular pathways to neurodegeneration in Alzheimer's disease and other disorders. *Nat Rev Neurosci.* 2011;12(12):723-738. doi:10.1038/nrn3114

10. McLeod DS, Lutty GA. High-resolution histologic analysis of the human choroidal vasculature. *Invest Ophthalmol Vis Sci.* 1994;35(11):3799-3811.

11. Cunha JP, Proença R, Dias-Santos A, et al. Choroidal thinning: Alzheimer's disease and aging. *Alzheimers Dement (Amst).* 2017;8:11-17. doi:10.1016/j.dadm.2017.03.004

12. Gharbiya M, Trebbastoni A, Parisi F, et al. Choroidal thinning as a new finding in Alzheimer's disease: evidence from enhanced depth imaging spectral domain optical coherence tomography. *J Alzheimers Dis.* 2014;40(4):907-917. doi:10.3233/JAD-132039

13. Trebbastoni A, Marcelli M, Mallone F, et al. Attenuation of choroidal thickness in patients with Alzheimer disease: evidence from an Italian prospective study. *Alzheimer Dis Assoc Disord.* 2017;31(2):128-134. doi:10.1097/WAD.0000000000000176

14. Asanad S, Ross-Cisneros FN, Barron E, et al. The retinal choroid as an oculovascular biomarker for Alzheimer's dementia: a histopathological study in severe disease. *Alzheimers Dement (Amst).* 2019;11:775-783. doi:10.1016/j.dadm.2019.08.005

15. Bulut M, Yaman A, Erol MK, et al. Choroidal thickness in patients with mild cognitive impairment and Alzheimer's type dementia. *J Ophthalmol.* 2016;2016:7291257. doi:10.1155/2016/7291257

16. Masellis M, Sherborn K, Neto P, et al. Early-onset dementias: diagnostic and etiological considerations. *Alzheimers Res Ther.* 2013;5(Suppl 1):S7. doi:10.1186/alzrt197

17. Nwadiugwu M. Early-onset dementia: key issues using a relationship-centred care approach. *Postgrad Med J.* 2021;97(1151):598-604. doi:10.1136/postgradmedj-2020-138517

18. Chiari A, Vinceti G, Adani G, et al. Epidemiology of early onset dementia and its clinical presentations in the province of Modena, Italy. *Alzheimers Dement.* 2021;17(1):81-88. doi:10.1002/alz.12177

19. Zhang S, Kwapong WR, Yang T, et al. Choriocapillaris changes are correlated with disease duration and MoCA score in early-onset dementia. *Front Aging Neurosci.* 2021;13:656750. doi:10.3389/fnagi.2021.656750

20. McKhann GM, Knopman DS, Chertkow H, et al. The diagnosis of dementia due to Alzheimer's disease: recommendations from the National Institute on Aging-Alzheimer's Association workgroups on diagnostic guidelines for Alzheimer's disease. *Alzheimers Dement.* 2011;7(3):263-269. doi:10.1016/j.jalz.2011.03.005

21. Jack CR Jr, Bennett DA, Blennow K, et al. NIA-AA research framework: toward a biological definition of Alzheimer's disease. *Alzheimers Dement.* 2018;14(4):535-562. doi:10.1016/j.jalz.2018.02.018

22. Mangiafico SP, Tuo QZ, Li XL, et al. Tau suppresses microtubule-regulated pancreatic insulin secretion. *Mol Psychiatry.* 2023;28(9):3982-3993. doi:10.1038/s41380-023-02267-w

23. Li H, Durbin R. Fast and accurate short read alignment with Burrows-Wheeler transform. *Bioinformatics.* 2009;25(14):1754-1760. doi:10.1093/bioinformatics/btp324

24. Li H, Handsaker B, Wysoker A, et al. The sequence alignment/map format and SAMtools. *Bioinformatics.* 2009;25(16):2078-2079. doi:10.1093/bioinformatics/btp352

25. Jiang L, Ding X, Wang W, Yang X, Li T, Lei P. Head-to-head comparison of different blood collecting tubes for quantification of Alzheimer's disease biomarkers in plasma. *Biomolecules.* 2022;12(9). doi:10.3390/biom12091194

26. Karran E, Mercken M, De Strooper B. The amyloid cascade hypothesis for Alzheimer's disease: an appraisal for the development of therapeutics. *Nat Rev Drug Discov.* 2011;10(9):698-712. doi:10.1038/nrd3505

27. Sperling RA, Aisen PS, Beckett LA, et al. Toward defining the preclinical stages of Alzheimer's disease: recommendations from the National Institute on Aging-Alzheimer's Association workgroups on diagnostic guidelines for Alzheimer's disease. *Alzheimers Dement.* 2011;7(3):280-292. doi:10.1016/j.jalz.2011.03.003

28. Quintana DD, Anantula Y, Garcia JA, et al. Microvascular degeneration occurs before plaque onset and progresses with age in 3xTg AD mice. *Neurobiol Aging.* 2021;105:115-128. doi:10.1016/j.neurobiolaging.2021.04.019

29. Park L, Koizumi K, El Jamal S, et al. Age-dependent neurovascular dysfunction and damage in a mouse model of cerebral amyloid angiopathy. *Stroke.* 2014;45(6):1815-1821. doi:10.1161/STROKEAHA.114.005179

30. Bell RD, Zlokovic BV. Neurovascular mechanisms and blood-brain barrier disorder in Alzheimer's disease. *Acta Neuropathol.* 2009;118(1):103-113. doi:10.1007/s00401-009-0522-3

31. Chum PP, Hakim MA, Behringer EJ. Cerebrovascular microRNA expression profile during early development of Alzheimer's disease in a mouse model. *J Alzheimers Dis.* 2022;85(1):91-113. doi:10.3233/JAD-215223

32. Liu J, Wan J, Kwapong WR, et al. Retinal microvasculature and cerebral hemodynamics in patients with internal carotid artery stenosis. *BMC Neurol.* 2022;22(1):386. doi:10.1186/s12883-022-02908-7

33. van Dinther M, Voorter PHM, Schram MT, et al. Retinal microvascular function is associated with the cerebral microcirculation as determined by intravoxel incoherent motion MRI. *J Neurol Sci.* 2022;440:120359. doi:10.1016/j.jns.2022.120359

34. Cabrera DeBuc D, Somfai GM, Koller A. Retinal microvascular network alterations: potential biomarkers of cerebrovascular and neural diseases. *Am J Physiol Heart Circ Physiol.* 2017;312(2):H201-H212. doi:10.1152/ajpheart.00201.2016

35. Mutlu U, Cremers LG, de Groot M, et al. Retinal microvasculature and white matter microstructure: the Rotterdam study. *Neurology.* 2016;87(10):1003-1010. doi:10.1212/WNL.0000000000003080

36. Koronyo Y, Biggs D, Barron E, et al. Retinal amyloid pathology and proof-of-concept imaging trial in Alzheimer's disease. *JCI Insight.* 2017;2(16):e93621. doi:10.1172/jci.insight.93621

37. Rissman RA, Trojanowski JQ, Shaw LM, Aisen PS. Longitudinal plasma amyloid beta as a biomarker of Alzheimer's disease. *J Neural Transm.* 2012;119(7):843-850. doi:10.1007/s00702-012-0772-4

38. Pais MV, Forlenza OV, Diniz BS. Plasma biomarkers of Alzheimer's disease: a review of available assays, recent developments, and implications for clinical practice. *J Alzheimers Dis Rep.* 2023;7(1):355-380. doi:10.3233/ADR-230029

39. Leuzy A, Mattsson-Carlgren N, Palmqvist S, Janelidze S, Dage JL, Hansson O. Blood-based biomarkers for Alzheimer's disease. *Embo Mol Med.* 2022;14(1):e14408. doi:10.15252/emmm.202114408

40. Song F, Poljak A, Valenzuela M, Mayeux R, Smythe GA, Sachdev PS. Meta-analysis of plasma amyloid-beta levels in Alzheimer's disease. *J Alzheimers Dis.* 2011;26(2):365-375. doi:10.3233/JAD-2011-101977

41. Meng J, Lei P. Plasma pTau181 as a biomarker for Alzheimer's disease. *MedComm (2020).* 2020;1(1):74-76. doi:10.1002/mco2.1

42. Ding X, Zhang S, Jiang L, Wang L, Li T, Lei P. Ultrasensitive assays for detection of plasma tau and phosphorylated tau 181 in Alzheimer's disease: a systematic review and meta-analysis. *Transl Neurodegener.* 2021;10(1):10. doi:10.1186/s40035-021-00234-5

43. Ding XL, Tuo QZ, Lei P. An introduction to ultrasensitive assays for plasma tau detection. *J Alzheimers Dis.* 2021;80(4):1353-1362. doi:10.3233/JAD-201499

44. Hase Y, Ding R, Harrison G, et al. White matter capillaries in vascular and neurodegenerative dementias. *Acta Neuropathol Commun.* 2019;7(1):16. doi:10.1186/s40478-019-0666-x

45. Wang Y, Rattner A, Zhou Y, Williams J, Smallwood PM, Nathans J. Norrin/Frizzled4 signaling in retinal vascular development and blood brain barrier plasticity. *Cell.* 2012;151(6):1332-1344. doi:10.1016/j.cell.2012.10.042

46. Linsenmeier RA, Braun RD. Oxygen distribution and consumption in the cat retina during normoxia and hypoxemia. *J Gen Physiol.* 1992;99(2):177-197. doi:10.1085/jgp.99.2.177

47. Birol G, Wang S, Budzynski E, Wangsa-Wirawan ND, Linsenmeier RA. Oxygen distribution and consumption in the macaque retina. *Am J Physiol-Heart C.* 2007;293(3):H1696-H1704. doi:10.1152/ajpheart.00221.2007

48. Bayhan HA, Aslan Bayhan S, Celikbilek A, Tanık N, Gürdal C. Evaluation of the chorioretinal thickness changes in Alzheimer's disease using

spectral-domain optical coherence tomography. *Clin Exp Ophthalmol.* 2015;43(2):145-151. doi:10.1111/ceo.12386

49. Cheung CY, Mok V, Foster PJ, Trucco E, Chen C, Wong TY. Retinal imaging in Alzheimer's disease. *J Neurol Neurosurg Psychiatry.* 2021;92(9):983-994. doi:10.1136/jnnp-2020-325347

50. Alber J, Goldfarb D, Thompson LI, et al. Developing retinal biomarkers for the earliest stages of Alzheimer's disease: what we know, what we don't, and how to move forward. *Alzheimers Dement.* 2020;16(1):229-243. doi:10.1002/alz.12006

51. Schmid JF, Müller K, Mühlemann J. Fallstricke Bei der Multidisziplinaren Behandlung Mehrfachverletzter [Pitfalls in the multidisciplinary treatment of the multiple injured]. *Z Unfallchir Versicherungsmed Berufskr.* 1985;78(1):41-45. .

52. Corradetti G, Oncel D, Kadomoto S, et al. Choriocapillaris and retinal vascular alterations in presymptomatic Alzheimer's disease. *Invest Ophthalmol Vis Sci.* 2024;65(1):47. doi:10.1167/iovs.65.1.47

53. Alber J, Bouwman F, den Haan J, et al. Retina pathology as a target for biomarkers for Alzheimer's disease: current status, ophthalmopathological background, challenges, and future directions. *Alzheimers Dement.* 2024;20(1):728-740. doi:10.1002/alz.13529

54. Touroutoglou A, Katsumi Y, Brickhouse M, et al. The sporadic early-onset Alzheimer's disease signature of atrophy: preliminary findings from the longitudinal early-onset Alzheimer's disease study (LEADS) cohort. *Alzheimers Dement.* 2023;19(Suppl 9):S74-S88. doi:10.1002/alz.13466

55. Aziz AL, Giusiano B, Joubert S, et al. Difference in imaging biomarkers of neurodegeneration between early and late-onset amnestic Alzheimer's disease. *Neurobiol Aging.* 2017;54:22-30. doi:10.1016/j.neurobiolaging.2017.02.010

56. Potsaid B, Baumann B, Huang D, et al. Ultrahigh speed 1050 nm swept source/Fourier domain OCT retinal and anterior segment imaging at 100,000 to 400,000 axial scans per second. *Opt Express.* 2010;18(19):20029-20048. doi:10.1364/OE.18.020029

57. Bell RD, Winkler EA, Singh I, et al. Apolipoprotein E controls cerebrovascular integrity via cyclophilin A. *Nature.* 2012;485(7399):512-516. doi:10.1038/nature11087

58. Koizumi K, Hattori Y, Ahn SJ, et al. Apoepsilon4 disrupts neurovascular regulation and undermines white matter integrity and cognitive function. *Nat Commun.* 2018;9(1):3816. doi:10.1038/s41467-018-06301-2

59. Kim JI, Kang BH. Decreased retinal thickness in patients with Alzheimer's disease is correlated with disease severity. *PLoS One.* 2019;14(11):e0224180. doi:10.1371/journal.pone.0224180

60. den Haan J, van de Kreeke A, Konijnenberg E, et al. Retinal thickness as a potential biomarker in patients with amyloid-proven early- and late-onset Alzheimer's disease. *Alzheimers Dement.* 2019;11:463-471. doi:10.1016/j.dadm.2019.05.002

61. Jáñez-Escalada L, Jañez-García L, Salobrar-García E, et al. Spatial analysis of thickness changes in ten retinal layers of Alzheimer's disease patients based on optical coherence tomography. *Sci Rep.* 2019;9:13000. doi:10.1038/s41598-019-49353-0

62. O'Bryhim BE, Apte RS, Kung N, Coble D, Van Stavern GP. Association of preclinical Alzheimer disease with optical coherence tomographic angiography findings. *JAMA Ophthalmol.* 2018;136(11):1242-1248. doi:10.1001/jamaophthalmol.2018.3556

SUPPORTING INFORMATION

Additional supporting information can be found online in the Supporting Information section at the end of this article.

How to cite this article: Kwapong WR, Tang F, Liu P, et al. Choriocapillaris reduction accurately discriminates against early-onset Alzheimer's disease. *Alzheimer's Dement.* 2024;20:4185–4198. https://doi.org/10.1002/alz.13871